CHARACTERISTICS OF PRESSURE PULSATIONS IN PIPING SYSTEMS EXCITED BY A CENTRIFUGAL COMPRESSOR

Itsuro HAYASHI
CHIYODA ADVANCED SOLUTIONS CORPORATION, Yokohama, Japan

Shigehiko KANEKO
THE UNIVERSITY OF TOKYO, Tokyo, Japan

ABSTRACT

To establish the practical evaluation method of the pressure pulsations excited by a centrifugal compressor or fan at blade passing frequency, a one-dimensional excitation source model for a compressor was proposed based on the equation of motion. The damping characteristics of the compressor were investigated experimentally and as a result, the resistance coefficient of the compressor depends on the Reynolds number defined by the equivalent velocity of the pulsating flow is introduced. It is also shown that the relation of the maximum pressure amplitude in piping systems to the location of the excitation source under resonant conditions can be evaluated by introducing the equivalent resistance of the compressor and that of piping systems.

1. NOMENCLATURE

A	: cross-sectional area of a pipe [m^2]
A_c	: equivalent area in a compressor [m^2]
c	: speed of sound [m/s]
D	: pipe diameter [m]
E	: damping energy [Nm]
F	: excitation force [N]
ℓ	: length of a piping element [m]
$\tilde{m}$	: mass flow rate [kg/s]
$\overline{m}$	: average mass flow rate [kg/s]
m	: fluctuation component of a mass flow rate [kg/s]
$\hat{m}$	: equivalent mass flow rate [kg/s]
p	: fluctuation component of pressure [Pa]
Δp	: pressure loss [Pa]
R	: equivalent resistance [kg/m^2s]
Re	: Reynolds number $\hat{u}D/\nu$ [-]
t	: time [s]
T	: cycle [s] （$T = 2\pi/\omega$）
$\overline{u}$	: average fluid velocity [m/s]
u	: fluctuation component of a fluid velocity [m/s]
$\hat{u}$	: equivalent fluid velocity [m/s]
Δx	: length of an excitation part in a compressor [m]
X_{com}	: compressor position from a pipe inlet [m]
ε	: damping energy per area [N/m]
λ	: friction factor for a pipe flow [-]
ν	: kinematic viscosity [m^2/s]
ρ	: fluid density [kg/m^3]
ω	: angular frequency [rad/s]
ζ	: damping coefficient of concentrated resistance [-]

SUFFIX

a	: amplitude
c	: excitation part in a compressor
d	: discharge side of an excitation part in a compressor
img	: imaginary part
in	: pipe inlet
out	: pipe outlet
p	: piping element
pip	: piping system
r	: concentrated resistance
real	: real part
s	: suction side of an excitation part in a compressor
t	: total system
α, β	: condition of the piping arrangement (See Fig.2)

2. INTRODUCTION

Severe noise and vibrations in piping systems are caused by pressure pulsations from a compressor or fan. In particular, the reduction of pressure pulsations at blade passing frequency is important for noise and vibration control of a centrifugal compressor or fan. Extensive research (Weidemann, 1971) was reported regarding blade passing sound / pulsation generated in a centrifugal fan, and similarity laws have been proposed (Neise, 1975). Although, the effect of the propagating passage was studied (Ohta et al, 1987), the characteristics of pressure pulsations under resonant conditions and the damping characteristics of the systems are not clear so far. Therefore, the evaluation method for pressure pulsations from a centrifugal compressor or fan in piping systems has not been established.

In this study, a one-dimensional excitation source model for a compressor was proposed based on the equation of motion. The relation between the resistance coefficient of the compressor and the operating point was investigated experimentally. As a result, the characteristics of pressure amplitude in piping systems under resonant conditions can be evaluated by this model taking into account the damping characteristics of the compressor.

3. SIMULATION MODEL

3.1 Excitation source model in a compressor

A one-dimensional model for the pressure excitation source in a compressor is shown in Fig.1. The excitation force is loaded to the fluid when blades are passing by a volute tongue. Pressure pulsations and mass flow rate fluctuations at suction / discharge side of an excitation part are obtained by

$$\frac{\partial m_{\mathrm{d}}}{\partial t}+\bar{u}\frac{\partial m_{\mathrm{d}}}{\partial x}+A_{\mathrm{c}}\frac{p_{\mathrm{d}}-p_{\mathrm{s}}}{\Delta x}+\frac{R_{\mathrm{t}}}{\Delta x}u_{\mathrm{d}}=\frac{F}{\Delta x}, \tag{1}$$

$$m_{\mathrm{d}}=m_{\mathrm{s}}-\frac{\partial p_{\mathrm{d}}}{\partial t}\cdot\frac{A_{\mathrm{c}}\Delta x}{C^{2}}, \tag{2}$$

$$R_{\mathrm{t}}=\frac{\zeta_{\mathrm{t}}}{2}\hat{m}. \tag{3}$$

Equation (1) is the equation of motion in the excitation part. Equation (2) is the continuity equation between the suction / discharge side of the excitation part. Transfer matrix method was used to calculate the pulsations in a pipe.

3.2 Damping model

Pulsation energy is attenuated due to losses in the compressor and piping elements. In particular, the pressure amplitude observed in the system is dominated by the system damping under resonant conditions. Therefore, the evaluation of damping is very important. In this study, the total system damping was evaluated by introducing the equivalent damping coefficient into Eq.(3). The equivalent mass flow rate in Eq.(3) is defined so as to dissipate the same energy as is lost by non-linear damping proportional to square velocity during one cycle of a pulsation (Matsuda and Hayama, 1985).

3.2.1 Concentrated resistance

Pressure losses by concentrated resistance at pipe inlet, pipe outlet, valves or orifices are given by

$$\Delta p_{\mathrm{r}}=\frac{\zeta_{\mathrm{r}}}{2\rho_{\mathrm{r}}A_{\mathrm{r}}{}^{2}}\left|\tilde{m}_{\mathrm{r}}\right|\tilde{m}_{\mathrm{r}}. \tag{4}$$

Accordingly, the energy loss per unit area due to concentrated resistance is obtained by

$$\varepsilon_{\mathrm{r}}=\int_{0}^{T}\Delta p_{\mathrm{r}}\cdot u_{\mathrm{r}}dt, \tag{5}$$

i.e. energy integral of Eq.(4). As a result, we derive

$$\varepsilon_{\mathrm{r}}=\frac{\zeta_{\mathrm{r}}}{2(\rho_{\mathrm{r}}A_{\mathrm{r}})^{2}A_{\mathrm{r}}}\cdot 2\overline{m}_{\mathrm{r}}m_{\mathrm{ra}}{}^{2}\frac{\pi}{\omega}, \tag{6}$$

by separating the mass flow rate into the average component and the fluctuation component as

$$\tilde{m}_{\mathrm{r}}=\overline{m}_{\mathrm{r}}+m_{\mathrm{ra}}\sin\omega t. \tag{7}$$

In Eq.(6), the fluctuation component of the mass flow rate is assumed to be less than the average mass flow rate at the same location. Based on Eq.(6), the energy loss by concentrated resistance in a piping system during one cycle of a pulsation is described by

$$E_{\mathrm{r}}=A_{\mathrm{r}}\cdot\varepsilon_{\mathrm{r}},$$

$$=\frac{\zeta_{\mathrm{r}}}{(\rho_{\mathrm{r}}A_{\mathrm{r}})^{2}}\frac{\pi}{\omega}\cdot\overline{m}_{\mathrm{r}}m_{\mathrm{ra}}{}^{2}. \tag{8}$$

3.2.2 Resistance by pipe friction

The pulsation energy loss due to pipe friction is calculated by taking the algebraic sum of the energy loss in each piping element as

$$E_{\mathrm{pip}}=\sum_{i=1}^{N}\frac{\lambda}{(\rho_{\mathrm{p}}A_{\mathrm{p}i})^{2}}\frac{\Delta\ell_{i}}{D_{i}}\frac{\pi}{\omega}\overline{m}_{\mathrm{p}i}m_{\mathrm{pa}i}{}^{2}, \tag{9}$$

in the same manner as section 3.2.1. In Eq.(9), the length of a piping element $\Delta\ell_i$ should be much shorter than the relevant wave length.

3.2.3 Resistance in a compressor

Assuming that the compressor resistance can be described in the same manner as concentrated resistance in a piping system, we derive

$$E_{c}=\frac{\zeta_{\mathrm{c}}}{(\rho_{\mathrm{c}}A_{\mathrm{c}})^{2}}\frac{\pi}{\omega}\overline{m}_{\mathrm{c}}m_{\mathrm{ca}}{}^{2}, \tag{10}$$

for pulsation energy loss in a centrifugal compressor. The evaluation method of ζ_c is described in chapter 4.

3.2.4 Equivalent damping

We evaluated the total damping in the compressor piping system by introducing the equivalent concentrated resistance at the excitation part in the compressor. More specifically, we evaluated the energy loss in the total system by the mass flow rate at the excitation part, assuming that the shape of the pressure distribution in the pipe is not changed by damping in each element. The energy loss in the total compressor piping system is obtained by

$$E_{\mathrm{t}}=E_{\mathrm{c}}+E_{\mathrm{r}}+E_{\mathrm{pip}}, \tag{11}$$

for one cycle of a pulsation.

Defining the equivalent resistance in the compressor as it loses the same energy as is lost in the total system for one cycle of a pulsation, we can describe the total energy loss as

$$E_{t}=\frac{\zeta_{t}}{(\rho_{c}A_{c})^{2}}\frac{\pi}{\omega}\cdot\overline{m}_{c}m_{ca}{}^{2}. \tag{12}$$

Therefore, substitution of Eq.(8), Eq.(9), Eq.(10)

and Eq.(12), into Eq.(11) yeilds the equivalent resistance in the compressor as

$$\zeta_t = \zeta_c + \zeta_{rin}\frac{(\rho_c A_c)^2}{(\rho_{rin}A_{rin})^2}\frac{\overline{m}_{rin}m_{rain}{}^2}{\overline{m}_c m_{ca}{}^2} + \zeta_{rout}\frac{(\rho_c A_c)^2}{(\rho_{rout}A_{rout})^2}\frac{\overline{m}_{rout}m_{raout}{}^2}{\overline{m}_c m_{ca}{}^2} + \sum_{i=1}^{N}\lambda\frac{\Delta\ell_i}{D_i}\frac{(\rho_c A_c)^2}{(\rho_p A_p)^2}\frac{\overline{m}_{pi}m_{pai}{}^2}{\overline{m}_c m_{ca}{}^2}. \quad (13)$$

4. EVALUATION METHOD OF DAMPING

4.1 Evaluation of the transfer matrix Z_2

The damping in the compressor was evaluated as a concentrated resistance in this study. We obtained the resistance coefficient of the compressor by assuming that the transfer matrix Z_2 of the compressor is in accordance with Z_2 of the equivalent pipe element, which is obtained by

$$p_d = \frac{1}{2}\left(e^{j\frac{\omega}{c}\sqrt{1-j\frac{\sigma}{\omega}}\cdot\ell} + e^{-j\frac{\omega}{c}\sqrt{1-j\frac{\sigma}{\omega}}\cdot\ell}\right)p_s - \frac{c\sqrt{1-j\frac{\sigma}{\omega}}}{A}\cdot\frac{1}{2}\left(e^{j\frac{\omega}{c}\sqrt{1-j\frac{\sigma}{\omega}}\cdot\ell} - e^{-j\frac{\omega}{c}\sqrt{1-j\frac{\sigma}{\omega}}\cdot\ell}\right)m_s = Z_1\cdot p_s + Z_2\cdot m_s. \quad (14)$$

In Eq.(14), the friction loss in the pipe is described as

$$\sigma = \frac{\lambda}{2D\rho A}\hat{m}. \quad (15)$$

On the other hand, the transfer matrix Z_2 of the compressor is expressed as

$$Z_2 = \frac{p_{d\beta}p_{s\alpha} - p_{d\alpha}p_{s\beta}}{m_{s\beta}p_{s\alpha} - m_{s\alpha}p_{s\beta}}, \quad (16)$$

which is obtained experimentally by measuring the pressure pulsations at suction / discharge side of the compressor for different piping conditions as shown in Fig.2. The fluctuation components of the mass flow rate were calculated by the transfer matrix method.

4.2 Evaluation of the resistance coefficient

The pressure loss due to the fluctuation of the mass flow rate is obtained by

$$\Delta p = \frac{\ell\sigma}{A}\cdot m, \quad (17)$$

for a pipe element and

$$\Delta p_c = \frac{\zeta_c}{2\rho_c A_c{}^2}\hat{m}\cdot m, \quad (18)$$

for a compressor. Therefore, assuming that the pressure loss in the equivalent pipe is equal to that of the compressor, we derive the resistance coefficient of the compressor as

$$\zeta_c = \frac{2\rho A\ell}{\hat{m}}\cdot\sigma. \quad (19)$$

In Eq.(19), we obtain the friction loss by assuming that the transfer matrix Z_2 in Eq.(14) is equal to that in Eq.(16).

5. EXPERIMENTAL CONDITION

Pressure pulsation amplitude in the piping system was measured experimentally to evaluate the damping in the compressor and to validate the simulation model. Figure 3 shows the experimental setup for the compressor piping system. The operating condition of the compressor was changed by controlling the valve at the nozzle of the drum. The combination of the suction and discharge pipe was changed so that the relative position of the compressor in the piping systems could be changed. The discharge drum was unattached, when the effect of the compressor position on the pressure pulsations were investigated. The rotational speed of the motor was controlled by the inverter from 10rps to 50rps. The number of impeller blade was five, thus the maximum blade passing frequency was 250Hz.

In order to obtain the resistance coefficient of the compressor, the system was acoustically loaded by the loud speaker set at the suction end.

6. RESULTS AND DISCUSSION

6.1 Transfer matrix Z_2 of the compressor

The operating points of the compressor are shown in Fig.4. The transfer matrix Z_2 of the compressor was obtained for operating point case1, case2 and case3, respectively. Figure 5 shows Z_2 for case1 as a representative of three cases. In Fig.5, both imaginary and real part of the Z_2 obtained by experiments are in good accordance with those obtained by the theory of the equivalent piping model. As a result, the proposed evaluation method of Z_2 for the compressor is validated.

6.2 Resistance coefficient of the compressor

Figure 6 shows the resistance coefficients of the

compressor for the different operating conditions. From Fig.6, it is shown that the operating point of the compressor did not affect on the resistance coefficient when the average flow rate was larger than the design point (case1 and case2). On the other hand, when the average flow rate was zero, the resistance coefficients for case3 were 1000 times larger than those for case1 and case2. These phenomena can be evaluated by using the equivalent mass flow rate $\hat{m}$. Figure 7 shows the relation between the resistance coefficients and the Reynolds Number Re defined by the equivalent velocity $\hat{u}$. In case3, the resistance coefficient increased as Reynolds Number decreased. More specifically, the resistance coefficient of the compressor was inversely proportional to the Reynolds Number in this region. This trend is similar to that of the friction factor λ of the pipe for a mean flow. A friction factor is inversely proportional to the Reynolds Number in a laminar flow region, while it is less dependent on the Reynolds Number in a turbulent flow region. As a consequence, the resistance coefficients of the compressor for a pulsating flow can be evaluated by the equivalent velocity in the compressor.

6.3 Pressure amplitude in the piping systems

Pressure response curves in the pipe obtained by experiment and simulation for the different operating points are shown in Fig.8, Fig.9, Fig.10 and Fig.11. For simulation, the parameters related to the excitation part in the compressor, such as the resistance coefficient and the excitation force, were determined by using the experimental results. Pressure amplitude was non-dimensionalized by dynamic pressure based on the tip velocity of the impeller. Figure 8, Fig.9 and Fig.10 indicate that the pressure amplitude in the pipe can be accurately evaluated by the proposed simulation model in the wide operating range including the no flow condition. Furthermore, the effect of the orifice plate on the reduction of the pressure amplitude can be evaluated by this model (Fig.11).

The relation of the maximum pressure amplitude in the piping system to the location of the compressor under resonant condition of the second mode is shown in Fig.12. As a result of experiment, the maximum pressure amplitude in the piping system increased as the location of the compressor was close to a node of the pressure distribution of the resonant mode. Although these phenomena are similar to those observed in a centrifugal pump system (Sano, 1984), the mechanism has not been clarified. The results of the simulation in Fig.12 show that the proposed simulation model can evaluate the relation of the maximum pressure amplitude in a piping system to the location of a compressor appropriately.

6.4 Role of the total system damping

To find out the factor dominates the relation of the maximum pressure amplitude to the location of the compressor at the resonant frequency, the equivalent resistance in the compressor was investigated. Figure 13 shows the relation between the equivalent resistance in the compressor and the position of the compressor for the second mode. Figure 13 indicates that the equivalent resistance increased as the location of the compressor was close to the anti-node of the pressure distribution of the resonant mode. Hence, the maximum pressure amplitude decreased when the location of the compressor was close to the anti-node of the pressure distribution of the resonant mode. In contrast, when the location of the compressor was close to the node of the pressure distribution of the resonant mode, the equivalent resistance decreased, and thus the maximum pressure amplitude increased. As a consequence, the relation of the maximum pressure amplitude at the resonant frequency to the compressor location can be evaluated by damping in the total piping system. Thus, damping characteristics of the total piping systems under resonant conditions are clarified.

7. CONCLUSION

The characteristics of pressure pulsations by a centrifugal compressor at the blade passing frequency in a piping system were studied by a one-dimensional wave model. As a result, the following conclusions are drawn:

1. The operating point of the compressor does not affect on the resistance coefficient when the average flow rate is larger than the design point.

2. The resistance coefficient of the compressor is inversely proportional to the Reynolds Number when Re is less than 100.

3. The pressure amplitude in the pipe can be accurately evaluated by the proposed simulation model in the wide operating range including the no flow condition.

4. The relation of the maximum pressure amplitude to the compressor location is dominated by the total system damping in a compressor piping system.

5. The total system damping can be evaluated as the equivalent resistance in the compressor.

8. REFERENCES

Matsuda, H., and Hayama, S., 1985, A Method for Calculating the Pressure Pulsations Taking Dynamic Compressor-Piping Interaction into Account, Bulletin of JSME **28**-245: 2707-2714

Neise, W., 1975, Application of Similarity Laws to the Blade Passage Sound of Centrifugal Fans, J. Sound Vib., **43**-1: 61-75

Ohta, Y., Outa, E., and Tajima, K., 1987, Characteristics of Blade Passing Frequency Noise of a Centrifugal Fan, and a Method for Noise Reduction, Trans. JSME, Series B, **54**-500: 890-899

(in Japanese)

Sano, M., 1984, Trans. JSME, Series B, **50**-458: 2316-2324 (in Japanese)

Weidemann, J., 1971, Analysis of The Relation between Acoustic and Aerodynamic Parameters for a Series of Dimensionally Similar Centrifugal Fan Rotors, NASA TT F-13: 793

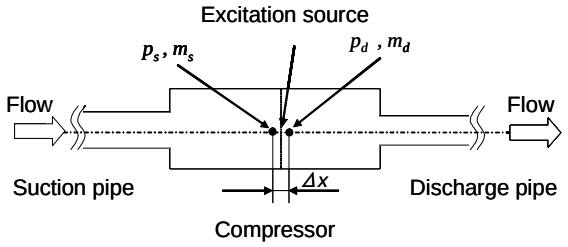

Figure 1: *Schematic representation of a pressure excitation source model of a compressor.*

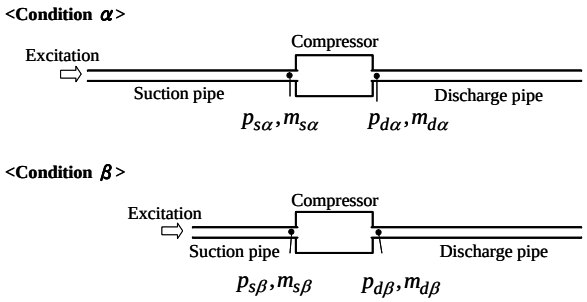

Figure 2: *Schematic representation of compressor piping systems.*

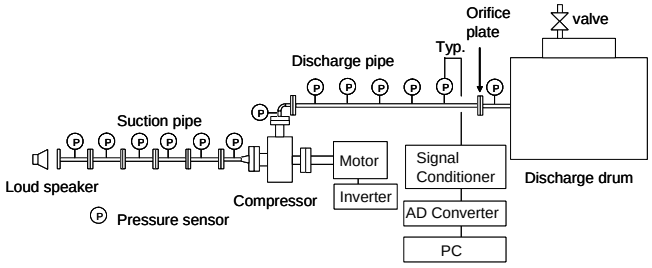

Figure 3: Experimental setup.

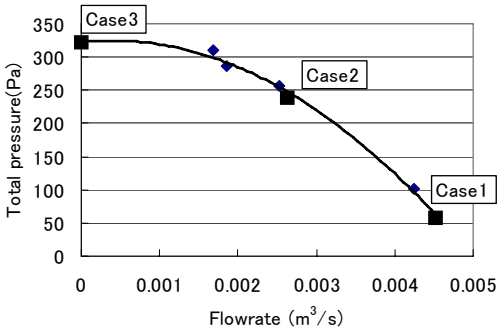

Figure 4: *Performance curve of the compressor.*

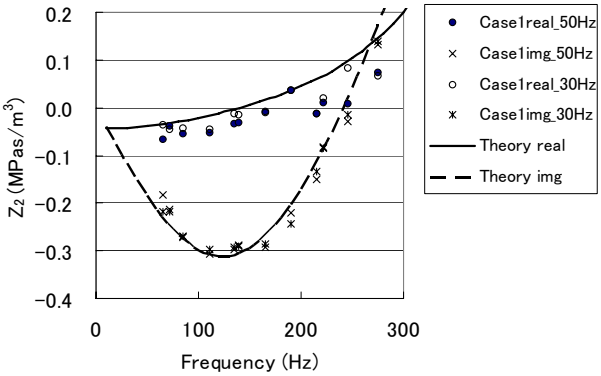

Figure 5: *Transfer matrix Z_2 of the compressor for Case 1.*

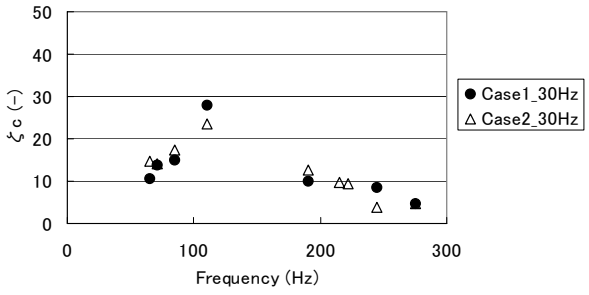

Figure 6: *Resistance coefficients of the compressor for Case 1 and Case 2.*

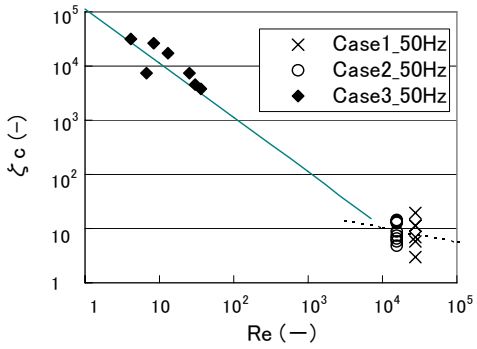

Figure 7: *Resistance coefficients of the compressor.*

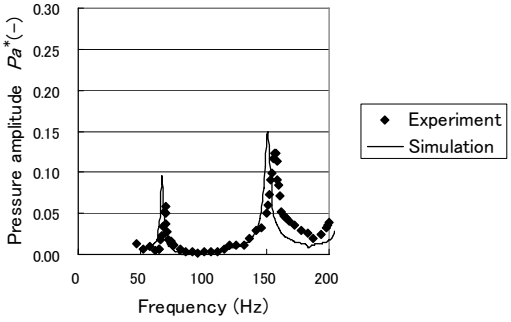

Figure 8: *The frequency response of pressure pulsations in the suction pipe for Case 1.*

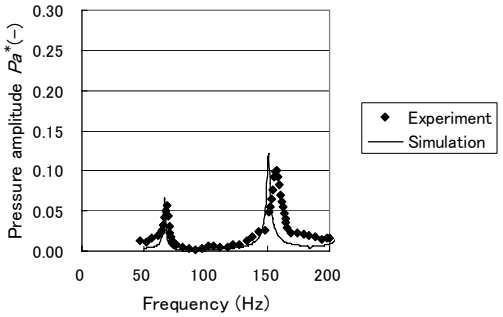

Figure 9: *The frequency response of pressure pulsations in the suction pipe for Case 2.*

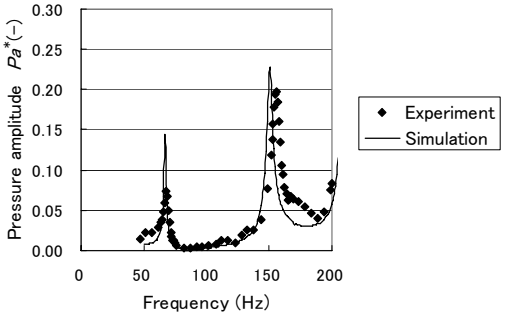

Figure 10: *The frequency response of pressure pulsations in the suction pipe for Case 3.*

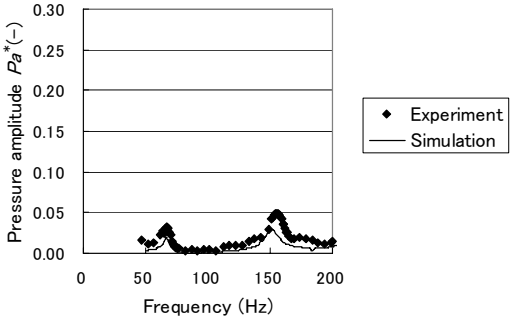

Figure 11: *The frequency response of pressure pulsations in the suction pipe for Case 2 with orifice plate.*

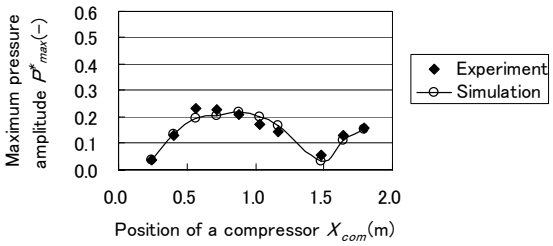

Figure 12: *The relation of the maximum pressure amplitude of the second mode in a pipe to the position of a compressor.*

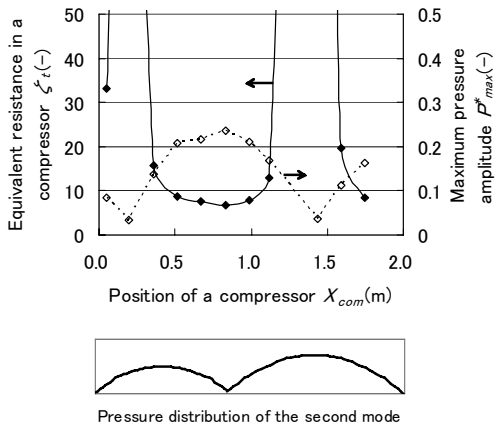

Figure 13: *The equivalent resistance in the compressor for the second mode. Lower graph is the pressure distribution of the second mode.*